RSC Advances

ROYAL SOCIETY OF CHEMISTRY

www.rsc.org/advances

Journal Name

COMMUNICATION

A novel synthesis of porous graphene nanoarchitectures using silver nanoparticles for fabricating enzyme sensor

Received 00th January 20xx,
Accepted 00th January 20xx

DOI: 10.1039/x0xx00000x

www.rsc.org/

Yidan Liu[a], Xiuhui Liu*[a], Ming Li[a], Yuelin Liu[a], Zhipan Guo[a], Zhonghua Xue[a], Xiaoquan Lu*[a]

In this communication we present the innovative synthesis of porous graphene (PGN) using silver nanoparticles (AgNPs) etching. The PGN material with large specific area and good biocompatible was used to load on great amount of enzyme, horseradish peroxidase (HRP), to fabricate an amperometric sensor. The constructed electrode displayed good electrocatalytic activity toward H_2O_2 reduction, and the peak current was 4.8 times as large as that of bare glassy carbon electrode. Moreover, the electrocatalytic mechanism of H_2O_2 reduction on HRP/PGN/GC electrode was also explored.

In 2004, as soon as graphene sheet was produced experimentally by mechanical exfoliation of graphite[1], it became the focus of scientific research immediately due to the unique properties[2-4]. It is possible to tailor the graphene properties and produce new types of graphene-based materials by modifying the structure of graphene (basal planes or edges). In recent years, more and more researchers have paid attention to the potential applications arising from the defects in the graphene sheets from a material science perspective, and it was found that much of the catalytic activity, electron transfer and chemical reactivity of graphene is at surface defect sites.[5]

Porous graphene (PGN), a kind of modified graphene sheet, can be described as a graphene sheet with some holes/pores within the atomic plane.[6,7] Due to its porous structure and more defects, PGN should be very useful as a new support matrix since it can not only provide large surface area, but also facilitate the diffusion and mass transport of reactants.[8-11] Thus, PGN could have potential applications for gas separation[12], water desalination[13], energy storage[14], fuel cells[15], electrochemical capacitors[16] and electrochemical sensors[17]. Some methods have been successfully developed to prepare porous graphene, such as "bottom-up" polymerization of a macrocycle[18], activation of exfoliated graphene oxide (GO) with KOH[19], hydrothermal steam etching of GO nanosheets[20], carbothermal etching[21], controlled catalytic oxidation[22], laser irradiation and electron beam irradiation[23]. But the costs of some methods mentioned above are prohibitive and the processes are too complicated and time-consuming. Therefore, it is essential to explore facile methods for the synthesis of PGN.

In this report, we described a novel and simple approach to fabricate the porous graphene by etching of graphene sheets using silver nanoparticles (AgNPs). Briefly, AgNPs-graphene nanocomposites were firstly prepared by a simple one-pot synthesis method. Next, the porous graphene could be obtained after the removal of AgNPs by treatment with nitric acid (HNO_3). Then we fabricated a novel enzymatic sensor of H_2O_2 utilizing the porous graphene as the matrix. Finally, the sensor displayed prominent electrocatalytic activity toward H_2O_2 reduction.

Graphene oxide (GO) dispersions were prepared from the graphite powder by a modified Hummers method.[24] The AgNPs-graphene nanocomposites were carried out by a facile and versatile hydrothermal synthetic strategy and the preparation steps are as follows: 0.06 g cetyltrimethylammonium bromide (CTAB) was initially dissolved into 12 mL water. Then CTAB solution was added into aqueous GO dispersion (1.0 $mg \cdot mL^{-1}$, 50mL), and the mixture was sonicated for 1 h, which achieve the CTAB-GO suspension. $NH_3 \cdot H_2O$ (3%) was dropped into aqueous $AgNO_3$ solution (0.02M, 5mL) continuously until the precipitates ($AgOH/Ag_2O$) disappeared and the Tollens' reagent [$Ag(NH_3)_2OH$] was obtained. Then the Tollens' reagent was dropped into as-synthesized CTAB-GO suspension and adequately stirred for 3 h in the atmosphere of nitrogen. Following this, 50 mL of $NaBH_4$ (40 mM) solution was added into the above mixture at a stirring rate of 600 rpm for 12 h at 80°C. The solution was filtered by nylon membrane with 0.22 μm pores, thoroughly washed with water to remove the free materials in the solution. The obtained black product, named as AgNPs-graphene (AgNPs-GN), was immersed in aqueous HNO_3 solution (1.0 M) and stirred for 4 days to

[a] Key Laboratory of Bioelectrochemistry & Environmental Analysis of Gansu Province, College of Chemistry & Chemical Engineering, Northwest Normal University, Lanzhou, 730070, China
†* Corresponding author. Tel.: +86 0931 7975276; fax: +86 0931 7971323. E mail: liuxh@nwnu.edu.cn
†* Corresponding author. Tel.: +86 0931 7971276; fax: +86 0931 7971323. E mail: luxq@nwnu.edu.cn

remove AgNPs. Thereafter, the porous graphene sample was collected by filtration and washed with water and ethanol. The product was obtained through freeze drying process. Finally, the H_2O_2 sensor was prepared as follows: a glassy carbon electrode (GCE) was polished with 1.0, 0.3 and 0.05 μm alumina slurry to a mirror-like, respectively, followed by rinsing thoroughly with doubly distilled water. Then 8μL of PGN aqueous solution (1.0 $mg \cdot mL^{-1}$) was dropped on the surface of a GCE and dried in air, and then the PGN/GCE was obtained. Next, horseradish peroxidase (HRP) (8μL, 1.0 $mg \cdot mL^{-1}$) was dropped on the PGN modified electrode and dried in air to obtain HRP/PGN/GCE.

The morphology and composition of the as-synthesised material were characterised by transmission electron microscopy, raman spectra, the nitrogen adsorption/desorption isotherm, X-ray diffraction and cyclic voltammetry. Transmission electron microscopy (TEM) was first used to characterize the morphologies of graphene oxide (GO), AgNPs-graphene nanocomposites (AgNPs-GN) and porous graphene (PGN). From Fig. 1A, it is clear that GO displays a typical 2D flake-like wrinkled shape. As shown in Fig. 1B, we can see that the spherical AgNPs with size of ~10 – 30nm were embedded in the graphene film by a one-pot reduction method. When AgNPs were removed by treatment with HNO_3, nano-scaled pores could be observed in Fig. 1C and Fig. 1D, validating PGN generation through AgNPs etching. In addition, the energy dispersive X-ray spectroscopy (EDX) was employed to assay their composition. As shown in inset of Fig. 1B, EDX of AgNPs-GN nanocomposites exhibit strong peaks of C, O and Ag, suggesting the formation of AgNPs-GN nanocomposites. While in inset of Fig. 1D, only peaks of C and O are observed in porous graphene, indicating an effective removel of AgNPs in the graphene by acid. By all account above, we may draw the conclusion that the porous graphene has been synthesized successfully.

Fig. 1

Another evidence for the introduction of pores on graphene sheets is the change of the D/G intensity ratio in Raman spectrum. As shown in Fig. 1E, the Raman spectrum of graphene-based materials displays two prominent peaks, corresponding to the D and G bands. The D band peak at 1348 cm^{-1} is corresponding to sp^3-hybridized carbon atoms on the defects and edges of the graphene sheets, while the G band at 1598 cm^{-1} represents the sp^2 in-plane vibration of carbon atoms[25]. Compared with GO (ID/IG=0.9), the porous graphene (PGN) samples exhibit larger D/G intensity ratio (ID/IG=1.1). Generally, the higher the D-band intensity, the more defects in graphene. Thus, the porous graphene has more defects, which are beneficial to the electron transfer of reactants and the chemical reactivity of graphene.

Moreover, the pore size determination and surface area of the porous graphene can be obtained by the nitrogen adsorption/desorption isotherm of it. Fig. 1F is the nitrogen adsorption/desorption isotherm of porous graphene, and its pore size distribution (inset). It is clear that the porous grahene posseses numerous mesopores with the average sizes of about 30 nm, which is consistent with the pore size from TEM (about 25 nm). Besides, the BET specific surface area of PGN (7067 m^2g^{-1}) is about 3 times higher than that of pure graghene (2630 m^2g^{-1}).

X-raydiffraction (XRD) analysis further confirms that porous graphene has been successfully prepared. In Fig. 2A, one can see that the prominent peaks in curve AgNPs-GN at 38.11°, 44.31°, 64.51°, and 77.51° are assigned to the (111), (200), (220), and (311) crystallographic planes of face-centered cubic (fcc) silver nanoparticles, respectively [JCPDS no. 01-087-0597].[26-30] However, these diffraction peaks of silver nanoparticles disappear in curve PGN, indicating porous graphene has been prepared successfully. These results are in accordance with TEM observation.

Fig. 2B shows cyclic voltammograms (CVs) obtained at bare GCE, AgNPs/GN/GCE and PGN/GCE in N_2-saturated 0.2 M PBS (pH 7.0). Compared with bare GCE (curve a), a sharp anodic peak at 0.43 V and a cathodic peak at 0.14 V were obtained in curve b, which were attributed to the oxidation of Ag and the reduction of Ag^+, proving the existence of AgNPs on the AgNPs/GN/GCE electrode. When the porous graphene (PGN) modified electrode was scanned in the same solution, as shown in curve c, we found that the redox peaks of Ag disappeared due to the removal of AgNPs by acid, and further confirmed porous graphene was modified on the electrode.

Fig. 2

PGN and HRP/PGN were separately applied to GC electrodes to investigate the reduction of hydrogen peroxide (H_2O_2). Fig. 2C shows the cyclic voltammograms at different modified electrodes in 1.0mM H_2O_2 and N_2 -saturated 0.2M PBS at pH 7.0. As shown in curve a, H_2O_2 was reduced irreversibly at a bare glassy carbon electrode at -0.64 V, which was attributed to the reduction of H_2O_2 to H_2O. When the porous graphene was modified on the surface of the electrode (curve b), the peak current increased a lot because PGN could provide large active area to contact H_2O_2 and facilitate its electron transfer. It was noticeable that when enzyme HRP was immobilized on the porous graphene, an excellent catalytic response signal was obtained in curve d, which was 4.8 times and 2.6 times as large as that of bare GCE (curve a) and PGN/GCE (curve b), respectively, revealing that HRP/PGN/GCE possesses the relatively remarkable catalytic ability to H_2O_2 reduction. Whereas, when enzyme HRP was immobilized on graphene (curve c), the peak current is also smaller than that of HRP/PGN/GCE (curve d), further indicating the good performance of the modified electrode toward H_2O_2 may result from the porous structure of graphene. The mechanism for H_2O_2 reduction reactions at the HRP/PGN/GCE was proposed as shown in Fig. 3.

Fig. 3

Generally, the reduction of H_2O_2 at the bare electrode was hardly achieved due to slow electrode kinetics and high overpotential, as shown in Eq. (1).[31,32] However, as the presence of the porous graphene and the enzyme HRP, the pores structure made the PGN become useful support matrix. On the one hand, PGN could load on great amount of HRP and offer a biocompatible microenvironment for retaining the HRP bioactivity. On the other hand, more electroactive sites of HRP, Fe^{III}, exposed on surface defect sites of the PGN modified electrode. When H_2O_2 diffuses from the solution to the electrode, Fe^{III} is oxidized first by H_2O_2 to produce an intermediate compound I (Fe^{IV}=O) as described in Eq. (2). Then compound I (Fe^{IV}=O) accepts one electron from the electrode and is reduced to form native HRP (Fe^{III}) again in Eq. (3). Finally, the circle of the oxidation/reduction would continue between Eq. (2) and (3), leading to a larger current signal on HRP/PGN/GCE. Therefore, the presence of the porous graphene plays an important role in the good performance of the sensor.

$$H_2O_2 + 2e^- + 2H^+ = 2H_2O \quad (1)$$

$$HRP\ (Fe^{III}) + H_2O_2 \rightarrow Compound\ I\ (Fe^{IV}{=}O) + H_2O \quad (2)$$

$$Compound\ I\ (Fe^{IV}{=}O) + 2H^+ + 2e^- \rightarrow HRP\ (Fe^{III}) + H_2O \quad (3)$$

In summary, a novel and facile approach to fabricate the porous graphene was exploited by AgNPs etching. The constructed enzymatic sensor based on porous graphene and the enzyme HRP displayed excellent electrocatalytic activity toward H_2O_2 reduction. Therefore, the present work provides a new ideal for the structural design a good biosensing platform and we believe that porous graphene materials should have high performance applications in the future.

Acknowledgments

This work was supported by the National Natural Science Foundation of China (Nos. 21565021 and 21265018), and Program for Chang Jiang Scholars and Innovative Research Team, Ministry of Education, China (Grant no. IRT1283).

References

1 K.S. Novoselov, A.K. Geim, S. Morozov, D. Jiang, Y. Zhang, S. Dubonos, I. Grigorieva and A. Firsov, Science. 2004, **306**, 666-669.
2 T. Ohta, A. Bostwick, T. Seyller, K. Horn and E. Rotenberg, Science. 2006, **313**, 951-954.
3 C.L. Kane and E.J. Mele, Phys. Rev. Lett. 2005, **95**, 226801.
4 M. Vozmediano, M. Lopez-Sancho, T. Stauber and F. Guinea, Phy. Rev. B. 2005, **72**, 155121.
5 C.E. Banks, T.J. Davies, G.G. Wildgoose and R.G. Compton, Chem. Commun. 2005, 829-841.
6 P. Russo, A. Hu and G. Compagnini, Nano-Micro Letters. 2013, **5**.
7 L. Jiang and Z. Fan, Nanoscale, 2014, **6**, 1922-1945.
8 M.A. Harmer, W.E. Farneth and Q. Sun, J. Am. Chem. Soc. 1996, **118**, 7708-7715.
9 H.D. Jang, H. Chang, K. Cho, F. Kim, K. Sohn and J. Huang, Aerosol Science and Technology. 2010, **44**, 1140-1145.
10 T. Hasell, C.D. Wood, R. Clowes, J.T. Jones, Y.Z. Khimyak, D.J. Adams and A.I. Cooper, Chem. Mater. 2009, **22**, 557-564.
11 S. Kim, Y. Kim, Y. Ko and J. Cho, J. Mater. Chem. 2011, **21**, 8008-8013.
12 D.-e. Jiang, V.R. Cooper and S. Dai, Nano lett. 2009, **9**, 4019-4024.
13 D. Cohen-Tanugi and J.C. Grossman, Nano lett. 2012, **12**, 3602-3608.
14 J. Zhu, D. Yang, X. Rui, D. Sim, H. Yu, H.E. Hoster, P.M. Ajayan and Q. Yan, Small. 2013, **9**, 3390-3397.
15 B. Sun, X. Huang, S. Chen, P. Munroe and G. Wang, Nano lett. 2014, **14**, 3145-3152.
16 T. Kyotani, Carbon, 2000, **38**, 269-286.
17 Q. Xi, X. Chen, D.G. Evans and W. Yang, Langmuir. 2012, **28**, 9885-9892.
18 M. Bieri, M. Treier, J. Cai, K. Aït-Mansour, P. Ruffieux, O. Gröning, P. Gröning, M. Kastler, R. Rieger and X. Feng, Chem. Commun. 2009, 6919-6921.
19 Y. Zhu, S. Murali, M.D. Stoller, K. Ganesh, W. Cai, P.J. Ferreira, A. Pirkle, R.M. Wallace, K.A. Cychosz and M. Thommes, Science, 2011, **332**, 1537-1541.
20 T.H. Han, Y.-K. Huang, A.T. Tan, V.P. Dravid and J. Huang, J. Am. Chem. Soc. 2011, **133**, 15264-15267.
21 D. Zhou, Y. Cui, P.-W. Xiao, M.-Y. Jiang and B.-H. Han, Nature communications. 2014, **5**.
22 Y. Lin, K. A. Watson, J. -W. Kim, D. W. Baggett, D. C. Working and J. W. Connell, Nanoscale, 2013, **5**, 7814-7824.
23 M.D. Fischbein and M. Drndić, Appl. Phys. Lett. 2008, **93**, 113107.
24 D. Li, M.B. Müller, S. Gilje, R.B. Kaner and G.G. Wallace, Nature nanotechnology. 2008, **3**, 101-105.
25 J. Xu, K. Wang, S.-Z. Zu, B.-H. Han and Z. Wei, ACS nano, 2010, **4**, 5019-5026.
26 J. Ma, J. Zhang, Z. Xiong, Y. Yong and X. Zhao, J. Mater. Chem. 2011, **21**, 3350-3352.
27 J. Shen, M. Shi, N. Li, B. Yan, H. Ma, Y. Hu and M. Ye, Nano research. 2010, **3**, 339-349.
28 T.T. Baby and S. Ramaprabhu, J. Mater. Chem. 2011, **21**, 9702-9709.
29 J.E. Song, T. Phenrat, S. Marinakos, Y. Xiao, J. Liu, M.R. Wiesner, R.D. Tilton and G.V. Lowry, Environmental science & technology. 2011, **45**, 5988-5995.
30 J. Tian, S. Liu, Y. Zhang, H. Li, L. Wang, Y. Luo, A.M. Asiri, A.O. Al-Youbi and X. Sun, Inorg. Chem. 2012,**51**, 4742-4746.
31 W. Zhao, H. Wang, X. Qin, X. Wang, Z. Zhao, Z. Miao,

L. Chen, M. Shan, Y. Fang and Q. Chen, Talanta, 2009, **80**, 1029-1033.
32 S. Thiagarajan, B.-W. Su and S.-M. Chen, Sensors and Actuators B: Chemical, 2009, **136**, 464-471.

Figure captions

Fig. 1. TEM images of GO (A), AgNPs-GN (B) and PGN (C, D); Insets are EDX images of AgNPs-GN (up) and PGN (down); Raman spectra of PGN and GO (E); Nitrogen adsorption/desorption isotherm and pore size distribution (inset) of PGN (F).

Fig. 2. (A) XRD patterns of PGN and AgNPs-GN; (B) Cyclic voltammograms of bare GCE (a) , AgNPs/GN/GCE (b) and PGN/GCE (c) in N_2 -saturated 0.2 M PBS (pH 7.0), at 50 mV/s; (C) Cyclic voltammograms of different electrodes in 1.0 mM H_2O_2 and N_2 -saturated 0.2 M PBS(pH 7.0): (a) bare GCE, (b) PGN/GCE, (c) HRP/GN/GCE (d) HRP/PGN/GCE at 50 mV/s.

Fig. 3. Schematic illustration of multi-step reactions at the enzyme biosensor.

Graphical Abstract

The porous graphene (PGN) using silver nanoparticles (AgNPs) etching has been successfully prepared in this work, and applied as electrode materials for enzyme sensor.

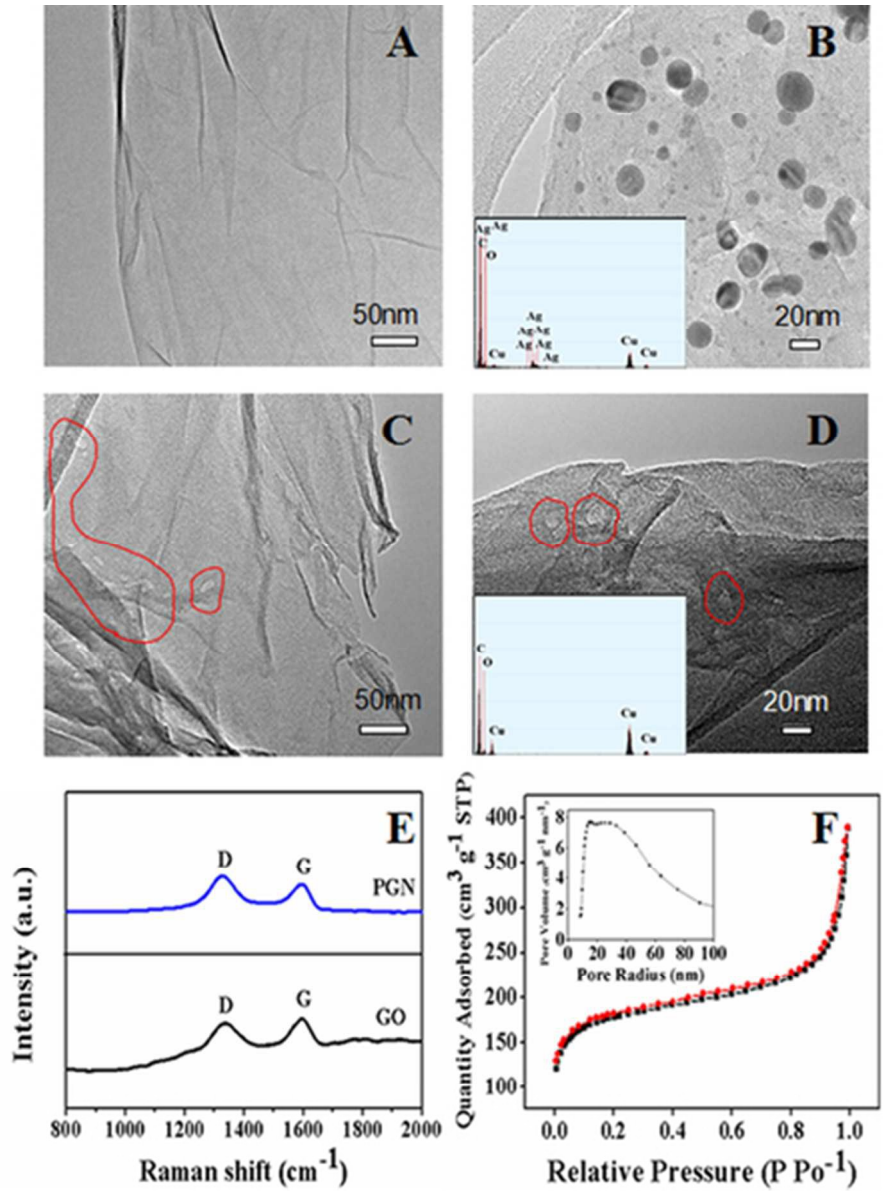

38x50mm (300 x 300 DPI)

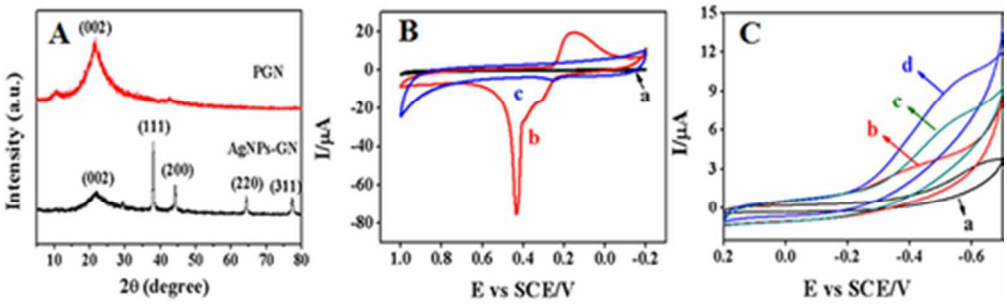

42x12mm (300 x 300 DPI)

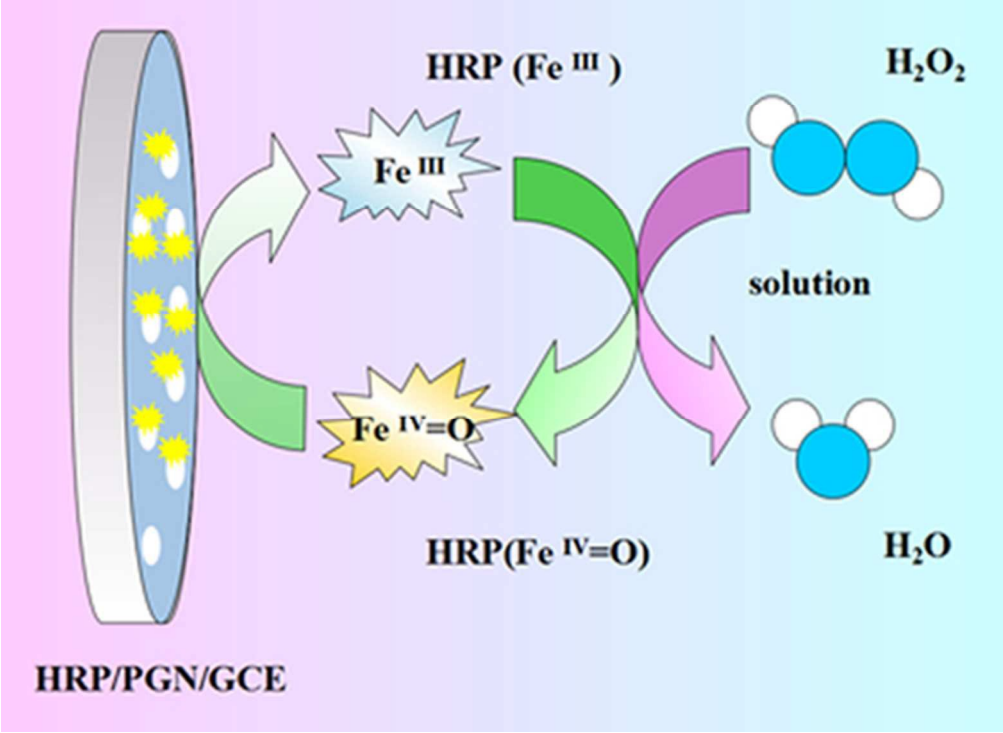

Fig. 3. Schematic illustration of multi-step reactions at the enzyme biosensor
43x32mm (300 x 300 DPI)

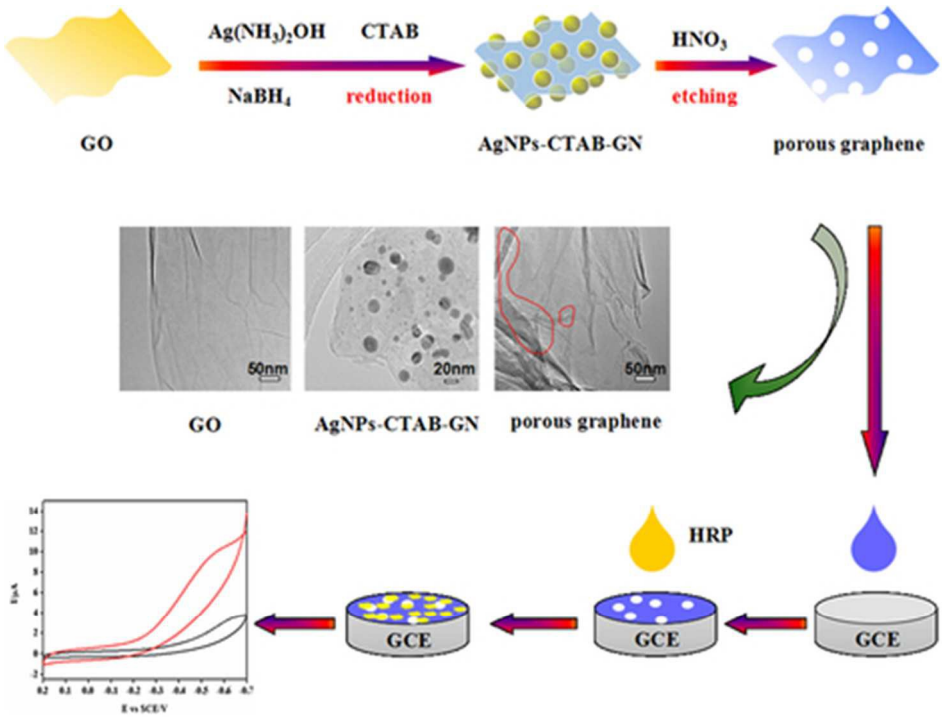

Graphical Abstract:The porous graphene (PGN) using silver nanoparticles (AgNPs) etching has been successfully prepared in this work, and applied as electrode materials for enzyme sensor
39x30mm (300 x 300 DPI)